Energy Storage

DOI: 10.1002/anie.201308354

Single-Layered Ultrasmall Nanoplates of MoS_2 Embedded in Carbon Nanofibers with Excellent Electrochemical Performance for Lithium and Sodium Storage**

Changbao Zhu, Xiaoke Mu, Peter A. van Aken, Yan Yu, and Joachim Maier**

Abstract: *The preparation and electrochemical storage behavior of MoS_2 nanodots—more precisely single-layered ultrasmall nanoplates—embedded in carbon nanowires has been studied. The preparation is achieved by an electrospinning process that can be easily scaled up. The rate performance and cycling stability of both lithium and sodium storage were found to be outstanding. The storage behavior is, moreover, highly exciting from a fundamental point of view, as the differences between the usual storage modes—insertion, conversion, interfacial storage—are beneficially blurred. The restriction to ultrasmall reaction domains allows for an almost diffusionless and nucleation-free "conversion", thereby resulting in a high capacity and a remarkable cycling performance.*

Molybdenum disulfide (MoS_2) has been widely used as a functional material in such diverse fields as lubrication,[1] electronic transistors,[2] batteries,[3] photovoltaics,[4] and catalysis.[5] Its unique mechanical, optical, and electrical properties are based on its chemical pecularities. MoS_2 is a layered transition-metal dichalcogenide (TMD) in which hexagonal layers of Mo are sandwiched between two S layers. Strong covalent bonding characterizes the Mo–S interactions, while the interactions between S layers are characterized by weak van der Waals interactions.[6] This gives rise to a pronounced layered situation similar to graphite, but with a different stacking sequence (see the Supporting Information S2). Single layers of MoS_2 have recently attracted great interest because of their modified properties compared to the bulk material.[2,7–12] There are several methods to synthesize single-layered or few-layered MoS_2, such as mechanical exfoliation,[13] chemical exfoliation,[14–16] hydrothermal synthesis,[17] and chemical vapor deposition.[18] However, finding an effective method which is simple and can be scaled up, has remained a challenge. Furthermore, the single-layered foils generated so far are rather extended, and if the lateral dimensions are reduced novel properties may arise as a consequence of edge effects or even quantum confinement effects. An equally fascinating point is the preparation of composites of single-layered plates with conducting and easily percolating partners, in particular by the inclusion of nanoplates in carbon nanofibers.

As a result of its pronounced redox variability and structural pecularities, MoS_2 is an attractive host for ion intercalation, in particular as the negative electrode in Li-based batteries.[3,19–22] Besides intercalation, MoS_2 can be converted into Mo and Li_2S with additional substantial gain in capacity. Li intercalation changes the Mo coordination from trigonal-prismatic to octahedral. The related change in the stacking sequence is opposite to that in graphite (see Supporting Information S2 and S3).

Some reports have demonstrated that the lithium storage capacity of MoS_2 can be further improved through structure modification, finally reaching a reversible capacity of 800–900 $\mathrm{mA\,h\,g^{-1}}$ at a low current rate.[23–27] There are two approaches to increase the specific capacity. The first one is to relax the strain and lower the barrier for lithium intercalation by preparing few-layered or even single-layered MoS_2 materials with different morphologies[19,23] (e.g. nanotube,[26] nanoflake[28]). However, in most cases, single-layered MoS_2 was not obtained, let alone single-layered plates of lateral nanodimensions. The other method is to synthesize carbon-coated MoS_2 or MoS_2-carbon composites[29] to enhance electron and mass transport.[30] Combining carbon nanotubes,[31] graphene,[20,32] or conductive polymers[3,24] with the poorly conductive MoS_2 was confirmed to be effective in this respect. However, the expensive and complex processing steps will limit the applicability of this approach.

The preparation of nanoplates is desired not only to increase lateral transport but also for the simple fact that MoS_2 shows a substantial volume change in the host matrix during cycling, usually leading to pulverization and aggregation of particles,[32] and hence poor cycling stability, especially at high discharge/charge rates. This is even more important when sodium storage is concerned, which currently attracts much attention because of the limited global resources of

---

[*] Prof. Y. Yu
CAS Key Laboratory of Materials for Energy Conversion
Department of Materials, Science and Engineering
University of Science and Technology of China
Hefei, 230026, Anhui (P. R. China)
E-mail: yanyumse@ustc.edu.cn

Dr. C. Zhu, Prof. Y. Yu, Prof. J. Maier
Max Planck Institute for Solid State Research
Heisenbergstrasse 1, 70569 Stuttgart (Germany)
E-mail: s.weiglein@fkf.mpg.de

Dr. X. Mu, Prof. P. A. van Aken
Max Planck Institute for Intelligent Systems
Heisenbergstrasse 3, 70569 Stuttgart (Germany)

[**] This work was financially supported by the Alexander von Humboldt Foundation (Sofja Kovalevskaja award), the National Natural Science Foundation of China (Nos. 21171015 and 21373195), the "1000 plan" of the Chinese Government and the program for New Century Excellent Talents in University (NCET), the Fundamental Research Funds for the Central Universities (WK2060140014), the Max Planck Society, as well as the European Union Seventh Framework Programme (FP7/2007-2013) under grant agreement no. 312483 (ESTEEM2).

Supporting information for this article is available on the WWW under http://dx.doi.org/10.1002/anie.201308354.

lithium. Considering the larger radius of Na^+ (0.102 nm) compared to Li^+ (0.076 nm), single-layered MoS_2 nanoplates in percolating carbon nanofibers should be well-suited for alleviating the mechanical stress resulting from the storage of the larger Na^+ ions and also for improving the performance. Herein, we report such a successful synthesis along with the outstanding electrochemical Li and Na storage properties.

Composites of single-layered MoS_2 nanoplates (thickness ca. 0.4 nm, lateral dimension ca. 4.0 nm) embedded in carbon nanofibers (ca. 50 nm) were prepared for the first time by electrospinning. The storage behavior of these nanodots is exciting, especially in terms of application purposes. Figure 1 a shows a schematic illustration of the typical electrospinning procedure with subsequent heat treatment. The X-ray diffraction (XRD) pattern (Figure 1 b) shows crystalline and single-phase MoS_2 with a hexagonal structure but no detectable impurities (JCPDS 37-1492). The absence of the (002) reflection that is typically observed in the bulk counterpart demonstrates the presence of "graphene-like" layers (i.e. less than five layers).[19,33] As shown in Figure 1 c,d, the MoS_2-carbon fibers are uniform, long, and continuous, connected with each other through the formation of a 3D network. Moreover, these nanofibers are very thin, with a diameter of around 50 nm, thus substantially thinner than the electrospun $LiFePO_4$ nanowires previously reported.[34] The carbon content of this composite is about 38 wt %, as measured by inductively coupled plasma atomic emission spectroscopy (ICP-AES).

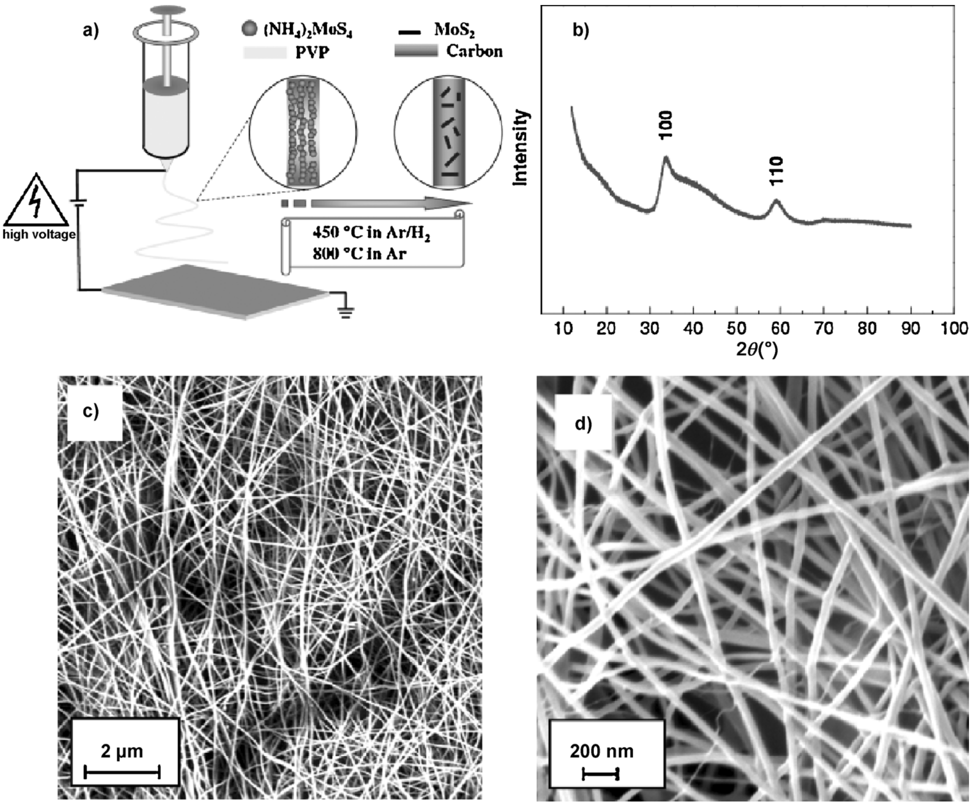

Figure 1. a) Schematic illustration of the electrospinning process to prepare single-layered MoS_2-carbon nanofiber composites. b) XRD pattern of such a composite. c),d) SEM images of such a composite at different magnifications. PVP = poly(vinylpyrrolidone).

Figure 2 a shows a transmission electron microscopy (TEM) bright-field (BF) image of such MoS_2-carbon composites, illustrating uniform nanofibers with diameters of about 50 nm, in good agreement with the scanning electron microscopy (SEM) images. The layers of MoS_2 are extremely thin and small, and are randomly embedded in the thin amorphous carbon fibers (Figure 2 b–d). The thickness of MoS_2 is 0.4 nm (Figure 2 d), which agrees with the spacing between the two S layers (sandwiching the Mo layer) as derived from bulk data (JCPDS 37-1492), hence indicating the presence of single-layered MoS_2. The lateral dimension of such a single-layered nanoplate is only around 4 nm. To the best of our knowledge, these are the smallest single-layered MoS_2 plates reported. This is not only exciting because of the extremely short perpendicular distances, but the lateral transport length will be tiny and the local electroactive mass will be small and extremely confined. This latter point will turn out to be most important for the reversibility of the "conversion" reactions. The 3D image of this unique morphology was obtained by TEM modeling studies (Figure 3;

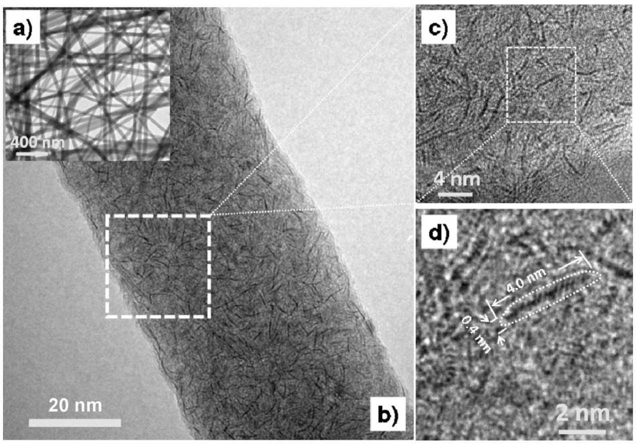

Figure 2. a) TEM-BF micrograph. b) HRTEM image showing the ultrathin MoS_2 embedded in the carbon nanofiber. c),d) Corresponding HRTEM images from the marked region in (b) and (c), respectively, to show the detailed structure of single-layered ultrasmall MoS_2 embedded in the amorphous carbon.

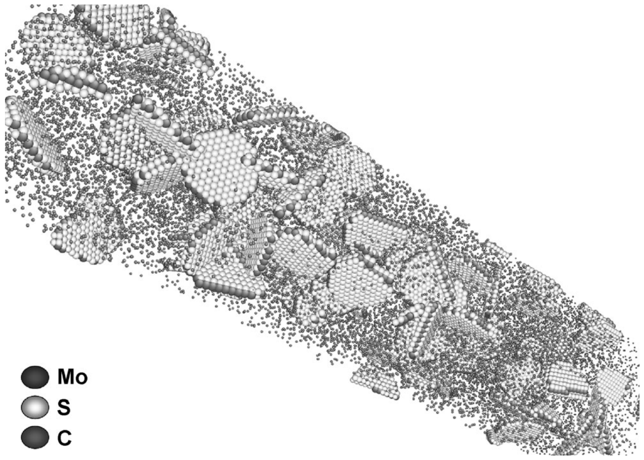

Figure 3. Schematic representation based on TEM modeling studies to demonstrate the unique morphology of such a composite: single-layered ultrasmall MoS_2 nanoplate embedded in a thin carbon nanofiber. The large black sphere, small black sphere, and white sphere correspond to Mo, C, and S, respectively.

the evolution mechanism of the morphology is discussed in Figure S6 in the Supporting Information).

The electrochemical performance in terms of lithium storage is outstanding (Figure 4). Figure 4a shows the discharge/charge profiles for the first three cycles at 100 $mA\,g^{-1}$ in the voltage window of 0.005 V to 3 V. The initial discharge and charge capacities are found to be 1712 and 1267 $mA\,h\,g^{-1}$, respectively, which corresponds to a Coulombic efficiency of 74%. Note that all the capacity values in this study refer to MoS_2. As our composite contains about 62 wt% MoS_2, the capacity data for the whole composite mass are excellent as well. (The values referring to the composite, carbon, and MoS_2 at various current densities are listed in the Supporting Information S4.) The irreversible capacity can mainly be attributed to electrolyte decomposition and the formation of a gel-like polymeric layer (solid electrolyte interface, SEI), as commonly observed at low potential for nanosized anode materials.[3] The Coulombic efficiency increases to 95.5% during the 2nd cycle, and further increases to 99.1% after 10 cycles. The remarkable rate performance is reflected by the specific capacity being around 1095, 986, 768, 637, 620, 548, and 374 $mA\,h\,g^{-1}$ when the current density increases from 0.5, 1, 5, 10, 20, 30, to 50 $A\,g^{-1}$, respectively, with good capacity retention as well (Figure 4b). Furthermore, the material exhibits excellent cycling stability at high current densities (Figure 4c). The capacity is 1007 $mA\,h\,g^{-1}$ after 100 cycles at a current density of 1 $A\,g^{-1}$, and still 661 $mA\,h\,g^{-1}$ even after 1000 cycles at a current density of 10 $A\,g^{-1}$.

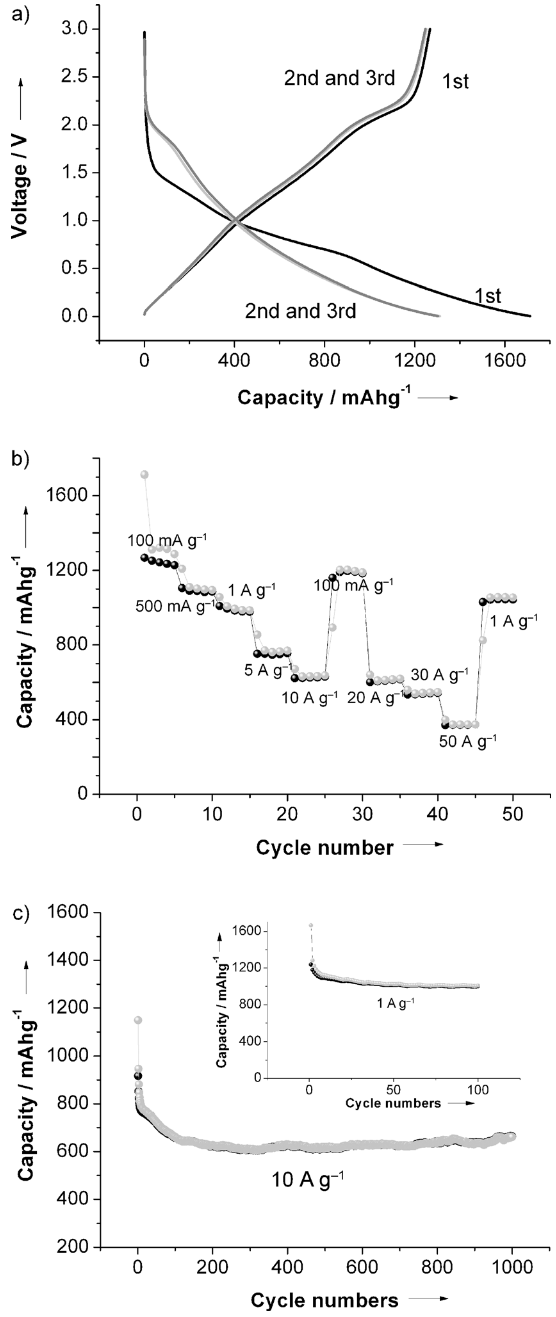

Figure 4. Excellent electrochemical performance of single-layered MoS_2-carbon nanofiber composite for lithium batteries. a) Charge and discharge voltage profiles for the first three cycles at 100 $mA\,g^{-1}$. b) High rate performance of such a composite. c) Excellent cycling performance. Black sphere: charge; gray sphere: discharge.

Moreover, we investigated the sodium storage behavior of the single-layered MoS_2/carbon nanowire composite (Figure 5). So far there is only one report available in the literature, solely referring to Na insertion in bulk materials.[35,36] By discharging to 0.005 V, we have the possibility to explore extensive sodium storage through a "conversion" reaction.[36] The discharge and charge profiles (Figure 5a) are similar to the curves for lithium storage, only with lower voltage and capacity, which is due to the difference in the thermodynamics and kinetics for the insertion of lithium and sodium ions. As a consequence of the larger ionic radius of Na^+ than Li^+,[37,38] the absolute values of Gibbs energy changes of storage reactions for Li are typically larger than for Na,[39] and the kinetics of sodium insertion and extraction are more sluggish compared to lithium. The Coulombic efficiency of the first cycle is 52% and increases to 98% for the third cycle. The excellent rate retention is shown in Figure 5b. The specific capacities are 854, 700, 623, 436, 331, 224, 155, and

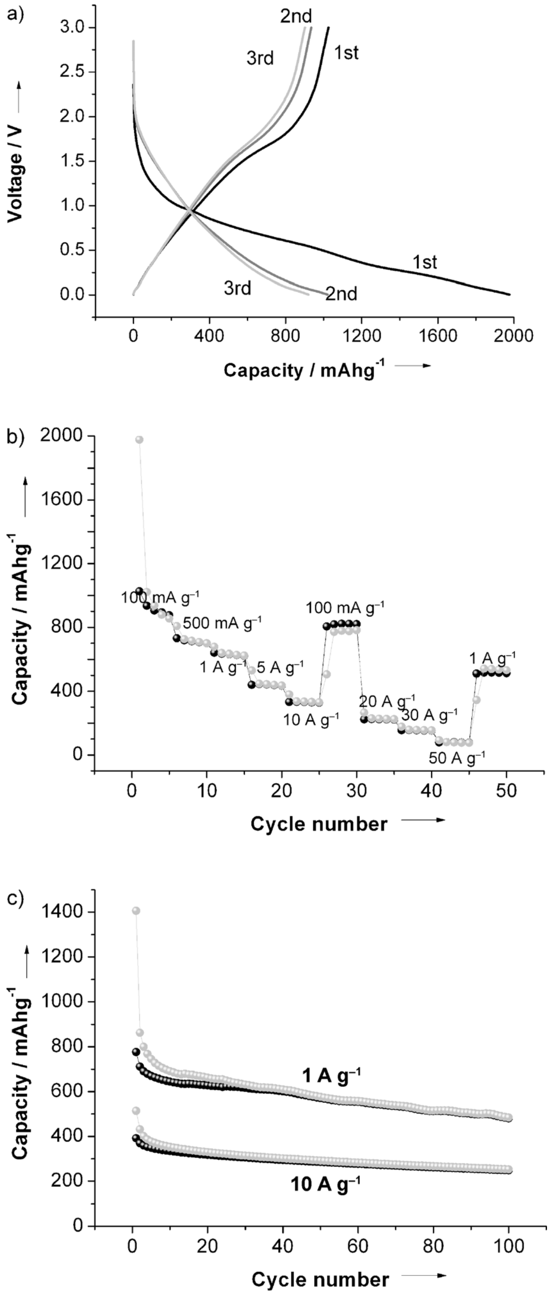

Figure 5. Excellent electrochemical performance of a single-layered MoS_2-carbon nanofiber composite for sodium batteries. a) Charge and discharge voltage profiles for the first three cycles at 100 mA g^{-1}. b) High rate performance of such a composite. c) Excellent cycling performance. Black sphere: charge; gray sphere: discharge.

75 mA h g^{-1} for current densities of 0.1, 0.5, 1, 5, 10, 20, 30, and 50 A g^{-1}, respectively. The comparable rate performance to that of lithium storage can again be attributed to the ultrasmall single-layered MoS_2. The cycling performance for sodium storage is also outstanding: after 100 cycles, the capacity is 484 mA h g^{-1} at a current density of 1 A g^{-1}, while the value is 253 mA h g^{-1} even at a current density of 10 A g^{-1} (Figure 5c). To our knowledge, this is the best rate performance and cycling stability for sodium storage in this material reported so far.

At this point it is pertinent to consider the extremely confined structure and discuss it in terms of usual storage mechanisms. If one deals with a single layer, differences between bulk storage and interfacial storage become naturally blurred. As far as kinetics are concerned, this point is very beneficial. Since we are dealing with a Mo layer sandwiched between two S layers, the usual intercalation degenerates to an interfacial storage. The fact that the characteristic voltages obtained from cyclovoltammetry curves (Figure S3 in the Supporting Information) are not significantly changed can be attributed to the not very dissimilar chemical environments (Li sited between sulfur and carbon atoms). As far as the kinetics are concerned, the tiny lateral dimension is very favorable here. Even more interesting is the issue of conversion, which in this case essentially means the final storage of four alkaline metal atoms per molybdenum and transfer of the outer electrons to form a Mo of zero valence. As a result of confinement in the matrix and the small local electroactive mass, the "products" will in the extreme case of a nanodot not be transported away to form separate metal and sulfide phases, and even nucleation may possibly not be necessary. This has two consequences: 1) The "conversion" voltage will be much smaller than that calculated from the macroscopic phase data (1.5 V). (This point is the prerequisite of being able to observe "insertion", which otherwise would be evaded by "conversion".) 2) The reversibility will be much greater as the reaction domains are minimal. Finally, it has to be kept in mind that further charge transfer to form a partially negatively charged Mo ($Li^{\delta+}$, $Mo^{\delta-}$) is possible (atomistic limit of the "job-sharing" mechanism involving Li/Mo), thus offering one explanation of the observed excess over the "theoretical" capacity.

The exciting perspective of a typically confined conversion is also mirrored in the energetics. The conversion voltage is substantially less than the value calculated from bulk thermodynamics. Assuming a symmetric polarization, an equilibrium value slightly above 1 V is expected. Since conversion reactions typically seem to show a substantially lower discharge polarization, we have to reckon with a realistic equilibrium value between 0.6 and 1 V (as compared to 1.5 V). It is shown in the Supporting Information S5 that such a shift can be easily understood by the small size of the reaction domains. (Two semiquantitative approaches are addressed there that lead to essentially the same results: bond breaking approach and capillary approach.) The fact that the conversion reaction voltage for bulk or multilayered MoS_2 is also low indicates that in these cases the size of the chemical domain (because of sluggish diffusion) is tiny and the reaction products are also confined.

Clearly, the outstanding rate performance and cycling stability for both lithium and sodium storage for this single-layered MoS_2/carbon nanowire composite can be ascribed to the unique nanostructure: 1) The single-layered nature allows for very efficient storage, not only by minimizing transport problems in the sulfide in all directions but also by reversibly "combining" interfacial storage, insertion, and conversion. 2) This is supported by spatial isolation in the carbon matrix and the lateral confinement. 3) The mechanical decoupling of the nanoplates nullifies the expansion (shrinkage) problems during charging (discharging). 4) The nanoplates are electrochemically perfectly coupled, as the carbon matrix is a very good mixed conductor (conductive for e^- and Li^+). 5) The 1D character of the carbon fibers makes ion access easy. 6) For the same geometrical reason, electron transport is excellent, a consequence of efficient percolation of the fibers. 7) The isolation of the nanoplates is not only beneficial by confining "products" of the deep discharge and rendering conversion reversible, it also prevents Ostwald ripening and coarsening. 8) Last but not least, the structure also offers advantages with respect to the formation of the solid electrolyte interface (SEI) passivation layer.[25]

In summary, for the first time, single-layered ultrasmall nanoplates of MoS_2 embedded in thin carbon nanowires were successfully prepared by electrospinning. For lithium storage, the capacity is 661 $mA\,h\,g^{-1}$ even after 1000 cycles at a high current density of 10 $A\,g^{-1}$. For sodium storage, a specific capacity of 854 $mA\,h\,g^{-1}$ is achieved at 0.1 $A\,g^{-1}$, and the capacity is 484 and 253 $mA\,h\,g^{-1}$ at 1 and 10 $A\,g^{-1}$, respectively, after 100 cycles. As far as we know, this is the best rate performance and cycling stability for sodium storage in MoS_2. The unique structure of the composite not only offers a perfect situation regarding the key parameters that determine rate performance, but storage in/at ultrathin nanoplates or generally in/at nanodots is, moreover, extremely exciting and efficient, as the extreme confinement of the reaction results in the classical storage modes becoming blurred and can be beneficially exploited, as seen by a pronounced cycling performance of the conversion reaction.

Received: September 24, 2013

Keywords: electrochemistry · energy storage · layered compounds · molybdenum · nanostructures

---

[1] M. Chhowalla, G. A. J. Amaratunga, *Nature* **2000**, *407*, 164.
[2] B. Radisavljevic, A. Radenovic, J. Brivio, V. Giacometti, A. Kis, *Nat. Nanotechnol.* **2011**, *6*, 147.
[3] Y. Shi, Y. Wang, J. I. Wong, A. Y. S. Tan, C.-L. Hsu, L.-J. Li, Y.-C. Lu, H. Y. Yang, *Sci. Rep.* **2013**, *50*, 2169.
[4] E. Gourmelon, O. Lignier, H. Hadouda, G. Couturier, J. C. Bernede, J. Tedd, J. Pouzet, J. Salardenne, *Sol. Energy Mater. Sol. Cells* **1997**, *46*, 115.
[5] H. I. Karunadasa, E. Montalvo, Y. Sun, M. Majda, J. R. Long, C. J. Chang, *Science* **2012**, *335*, 698.
[6] H. S. S. Ramakrishna Matte, A. Gomathi, A. K. Manna, D. J. Late, R. Datta, S. K. Pati, C. N. R. Rao, *Angew. Chem.* **2010**, *122*, 4153–4156; *Angew. Chem. Int. Ed.* **2010**, *49*, 4059.
[7] G. L. Frey, S. Elani, M. Homyonfer, Y. Feldman, R. Tenne, *Phys. Rev. B* **1998**, *57*, 6666.
[8] Y. Li, Z. Zhou, S. Zhang, Z. Chen, *J. Am. Chem. Soc.* **2008**, *130*, 16739.
[9] C. Zhu, Z. Zeng, H. Li, F. Li, C. Fan, H. Zhang, *J. Am. Chem. Soc.* **2013**, *135*, 5998.
[10] J. V. Lauritsen, J. Kibsgaard, S. Helveg, H. Topsoe, B. S. Clausen, E. Laegsgaard, F. Besenbacher, *Nat. Nanotechnol.* **2007**, *2*, 53.
[11] K. F. Mak, C. Lee, J. Hone, J. Shan, T. F. Heinz, *Phys. Rev. Lett.* **2010**, *105*, 136805.
[12] K. K. Kam, B. A. Parkinson, *J. Phys. Chem.* **1982**, *86*, 463–467.
[13] K. S. Novoselov, D. Jiang, F. Schedin, T. J. Booth, V. V. Khotkevich, S. V. Morozov, A. K. Geim, *Proc. Natl. Acad. Sci. USA* **2005**, *102*, 10451.
[14] R. A. Gordon, D. Yang, E. D. Crozier, D. T. Jiang, R. F. Frindt, *Phys. Rev. B* **2002**, *65*, 125407.
[15] R. J. Smith, P. J. King, M. Lotya, C. Wirtz, U. Khan, S. De, A. O'Neill, G. S. Duesberg, J. C. Grunlan, G. Moriarty, J. Chen, J. Wang, A. I. Minett, V. Nicolosi, J. N. Coleman, *Adv. Mater.* **2011**, *23*, 3944.
[16] P. Joensen, R. F. Frindt, S. R. Morrison, *Mater. Res. Bull.* **1986**, *21*, 457.
[17] Y. Tian, Y. He, Y. Zhu, *Mater. Chem. Phys.* **2004**, *87*, 87.
[18] Y. Zhan, Z. Liu, S. Najmaei, P. M. Ajayan, J. Lou, *Small* **2012**, *8*, 966.
[19] H. Hwang, H. Kim, J. Cho, *Nano Lett.* **2011**, *11*, 4826.
[20] K. Chang, D. Geng, X. Li, J. Yang, Y. Tang, M. Cai, R. Li, X. Sun, *Adv. Energy Mater.* **2013**, *3*, 839.
[21] J. Xiao, X. Wang, X.-Q. Yang, S. Xun, G. Liu, P. K. Koech, J. Liu, J. P. Lemmon, *Adv. Funct. Mater.* **2011**, *21*, 2840.
[22] H. Liu, D. Su, R. Zhou, B. Sun, G. Wang, S. Z. Qiao, *Adv. Energy Mater.* **2012**, *2*, 970.
[23] K. Chang, W. Chen, L. Ma, H. Li, H. Li, F. Huang, Z. Xu, Q. Zhang, J.-Y. Lee, *J. Mater. Chem.* **2011**, *21*, 6251.
[24] L. Yang, S. Wang, J. Mao, J. Deng, Q. Gao, Y. Tang, O. G. Schmidt, *Adv. Mater.* **2013**, *25*, 1180.
[25] X. Zhou, L.-J. Wan, Y.-G. Guo, *Chem. Commun.* **2013**, *49*, 1838.
[26] C. Zhang, Z. Wang, Z. Guo, X. W. Lou, *ACS Appl. Mater. Interfaces* **2012**, *4*, 3765.
[27] J.-Z. Wang, L. Lu, M. Lotya, J. N. Coleman, S.-L. Chou, H.-K. Liu, A. I. Minett, J. Chen, *Adv. Energy Mater.* **2013**, *3*, 798.
[28] C. Feng, J. Ma, H. Li, R. Zeng, Z. Guo, H. Liu, *Mater. Res. Bull.* **2009**, *44*, 1811.
[29] X. Zhou, L.-J. Wan, Y.-G. Guo, *Nanoscale* **2012**, *4*, 5868.
[30] G. González, M. A. Santa Ana, E. Benavente, *Electrochim. Acta* **1998**, *43*, 1327.
[31] K. Bindumadhavan, S. K. Srivastava, S. Mahanty, *Chem. Commun.* **2013**, *49*, 1823.
[32] Y. Gong, S. Yang, Z. Liu, L. Ma, R. Vajtai, P. M. Ajayan, *Adv. Mater.* **2013**, *25*, 3979.
[33] Q. Wang, J. Li, *J. Phys. Chem. C* **2007**, *111*, 1675.
[34] C. Zhu, Y. Yu, L. Gu, K. Weichert, J. Maier, *Angew. Chem.* **2011**, *123*, 6402; *Angew. Chem. Int. Ed.* **2011**, *50*, 6278.
[35] J. Park, J.-S. Kim, J.-W. Park, T.-H. Nam, K.-W. Kim, J.-H. Ahn, G. Wang, H.-J. Ahn, *Electrochim. Acta* **2013**, *92*, 427.
[36] S. Hariharan, K. Saravanan, V. Ramar, P. Balaya, *Phys. Chem. Chem. Phys.* **2013**, *15*, 2945.
[37] S.-W. Kim, D.-H. Seo, X. Ma, G. Ceder, K. Kang, *Adv. Energy Mater.* **2012**, *2*, 710.
[38] V. Palomares, P. Serras, I. Villaluenga, K. B. Hueso, J. Carretero-Gonzalez, T. Rojo, *Energy Environ. Sci.* **2012**, *5*, 5884.
[39] It is not appropriate to solely explain this by the typically lower Li^+/Li or Na^+/Na standard potential, as this involves the difference in the solvation energies that cancel in the free enthalpy change of the cell reaction.